Water Stability and Cytotoxic Activity Relationship of a Series of Ferrocenium Derivatives. ESR Insights on the Radical Production during the Degradation Process†

Giovanni Tabbì,‡ Claudio Cassino,§ Giorgio Cavigiolio,§ Donato Colangelo,|| Annalisa Ghiglia,|| Ilario Viano,|| and Domenico Osella*,§

Istituto di Biostrutture e Bioimmagini, CNR, Sezione di Catania, viale A. Doria 6, I-95125, Catania, Italy, Dipartimento di Scienze e Tecnologie Avanzate, Università del Piemonte Orientale "A. Avogadro", corso Borsalino 54, I-15100, Alessandria, Italy, and Dipartimento di Scienze Mediche, Università del Piemonte Orientale "A. Avogadro", via Solaroli 17, I-28100, Novara, Italy

Received July 30, 2002

The cytotoxicity of some ferrocenium salts and the lack of activity of the corresponding ferrocenes has been already demonstrated. The cytotoxic activity in different conditions of decamethylferrocenium tetrafluoroborate ($DEMFc^+$) in comparison with four other ferrocenium derivatives on MCF-7 cell line is reported. The relative stability in aqueous solutions with different buffering agents is investigated by means of UV−vis spectroscopy and correlated to the cytotoxic properties of the compounds. $DEMFc^+$, the most stable compound, shows the highest efficiency in inhibiting cell growth (IC_{50} 35 μM, for 48 h treatment). Relaxation time measurements point out the involvement of water molecules in the degradation process. ESR results confirm the ability of ferrocenium cations to produce oxygen radical species as a consequence of their degradation in water. Oxygen-dependent formation of both hydroxyl and superoxide radicals is established by the spin-trapping technique. A direct evidence of the $DEMFc^+$ radical production into the viable cells is obtained by means of fluorescence-activated cell sorter (FACS) analysis that reveals a dose-dependent growth of 8-oxoguanine, the initial product of the guanine oxidation. This DNA oxidative stress justifies the cytotoxic effect of $DEMFc^+$. Furthermore, the cytotoxic cooperative effect of bleomycin, an iron-dependent antitumor drug, and $DEMFc^+$ has been tested. We have demonstrated the synergic effect between the two drugs, that is explained by the complementary oxidative damage inflicted to DNA as well as by the increasing of bleomycin activation by the iron(II/III) species available in the cell compartment from ferrocenium degradation.

Introduction

The lack of activity of bis-cyclopentadienyl iron(II) (ferrocene) is well established in the literature.[1−3] Increasing its water solubility either by derivatization with polar substituents or by inclusion in cyclodextrins did not lead to better results.[4,5] On the other hand, there is a general agreement on in vivo antitumor activity of ferrocenium salts, indicating that only the compounds with iron in +3 oxidation state are able to trigger the toxic events.[2,3,5,6] In vitro studies confirmed the cytotoxicity of these compounds, pointing out different activities, depending on the nature of the cell lines employed.[4−8]

All previous studies invoked the instability of ferrocenium compounds in aqueous solutions, but few investigations dealt with this particular problem. Only the stability of 1,1′-dimethylferrocenium tetrafluoroborate, compared to that of ferrocenium tetrafluoroborate, was reported.[9] We evaluated the stability of five different ferrocenium compounds (see Scheme 1) under physiological conditions by means of spectroscopic and relaxometric techniques as well as their cytotoxic activity by in vitro assay using MCF-7 cell line.

In a previous work[5] we stated that $CAFc^+$ in aqueous solutions was able to produce free radicals, likely responsible for its antitumor activity. Moreover an indirect evidence of DNA cleavage by ferrocenium cations, suggesting the participation of $^{\bullet}OH$ was obtained by the thiobarbituric acid method.[10] To get further information on the radical species involved in the cytotoxic mechanism, we recorded ESR spectra of solutions containing either $DEMFc^+$ or Fc^+, under physiological conditions, using the spin-trapping technique. Furthermore, we quantified in vitro the amount of 8-oxoguanine in viable cells, a sensitive marker for DNA damage caused by reactive oxygen species (ROS).[11]

The clinically used antitumor drug bleomycin is known to be activated in the presence of iron. In particular, the activated bleomycin adduct (BLM*), responsible for the final oxidative DNA damage, carries a superoxide fragment coordinated to the iron(III) complexed by bleomycin. BLM* can be produced starting from either Fe(II) or Fe(III), through different

† This article includes material presented at the 1st International Symposium on Bio-organometallic Chemistry, Paris, France, July 18-20, 2002.

* Corresponding author: Tel.: +39-0131-287429. Fax: (internat.) +39-0131-287416. E-mail: domenico.osella@mfn.unipmn.it.

‡ IBB, CNR.

§ Dipartimento di Scienze e Tecnologie Avanzate, Università del Piemonte Orientale.

|| Dipartimento di Scienze Mediche, Università del Piemonte Orientale.

10.1021/jm021003k CCC: $22.00
Published on Web 11/22/2002

Scheme 1

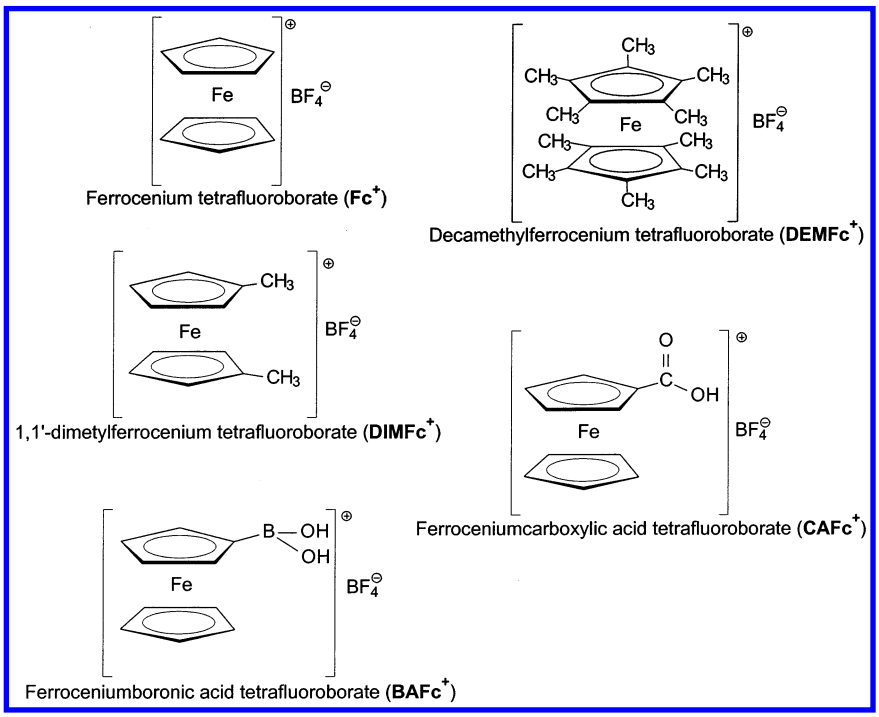

pathways involving different oxygen species.[12] The degradation process of ferrocenium salts in different solvents has been fully characterized by Prins et al.,[13] who have demonstrated that both Fe(II) and Fe(III) ions are formed during the degradation. Consequently, we have evaluated the potential synergy as cytotoxic of $DEMFc^+$ and bleomycin on MCF-7 cell line.

Results

Five different ferrocenium compounds were synthesized by chemical oxidation (see Experimental Section) of the corresponding ferrocene derivatives. The stability of these compounds in aqueous buffer solutions was evaluated by means of two different techniques: UV−vis spectroscopy and proton relaxation.

UV−vis Spectra. The UV−vis spectra were recorded as a function of the time (from 0 to 3000 min) using four different aqueous media: phosphate-citrate buffer at pH 3, freshly distilled water (pH ≈ 6.0−6.5), phosphate buffer at pH 7.4, and HEPES buffer at pH 7.4. This study was aimed to evaluate roughly the effect of the pH value and of the nature of the buffering agent on the degradation of the compounds. The decomposition of the complexes was followed by the decrease of the LMCT absorbance band ($1e_{1u} \rightarrow 2e_{1g}$),[14] which falls in the 250−300 nm range.

Fc^+ (Figure 1A) was unstable in all the media utilized; both the pH value, and the type of the buffering agent did not seem to stabilize this compound in solution. $DEMFc^+$ (Figure 1B) displayed the greatest stability among the tested compounds under all the conditions used. $DIMFc^+$ (Figure 1C) showed a stability trend between those of Fc^+ and $DEMFc^+$ up to 500 min after its dissolution. At longer times it exhibited a deeper decrease of the absorbance at 257 nm in acidic media (phosphate-citrate buffer and distilled water). The two acid derivatives [$CAFc^+$ (Figure 1D), $BAFc^+$ (Figure 1E)] showed a stability which is highly dependent on the pH value: they were generally stable under quite acidic conditions only.

Relaxation Measurements. We measured the paramagnetic contribution to the longitudinal relaxation time (T_{1p}) and the corresponding relaxation rate (R_{1p}) of water protons in the presence of the ferrocenium salts. Measurements were carried out in distilled water to rule out any buffer influence. Ferrocenium cations are able to increase the relaxation rate of the solvent molecules, being paramagnetic with an unpaired electron. This technique provides two kinds of information: (a) the ability of the water molecules to interact with the paramagnetic iron(III); (b) a direct evaluation of the stability of the compounds. According to Prins et al.[13] the ferrocenium degradation process in water leads mainly to the formation of iron(III) aquo ions. These d^5 high-spin ions cause a tremendous increase of the relaxation rate of water molecules. As a consequence, the extent of the degradation process can be followed by the increase of R_{1p} as a function of time.

It is well-known that Fe(III)EDTA (EDTA = ethylenediaminetetraacetic acid) has a water molecule in the first coordination sphere, whereas, in Fe(III)DTPA (DTPA = diethylenetriaminepentaacetic acid), the water molecules are located in the outer coordination sphere only.[15] To know whether the water molecules can coordinate to the iron center in the ferrocenium salts, their R_{1p} values were compared to those of the two reference complexes Fe(III)EDTA and Fe(III)DTPA. (see Table 1)

The R_{1p} values of all the ferrocenium cations were lower than that of the two reference complexes, thus indicating outer sphere interactions only.

Ferrocenium compounds carrying polar groups showed higher R_{1p} values compared with Fc^+; on the contrary, the methyl-substituted compounds exhibited lower relaxation rates. The hydrophilicity (polar substituent) or hydrophobicity (CH_3 substituent) affected the local

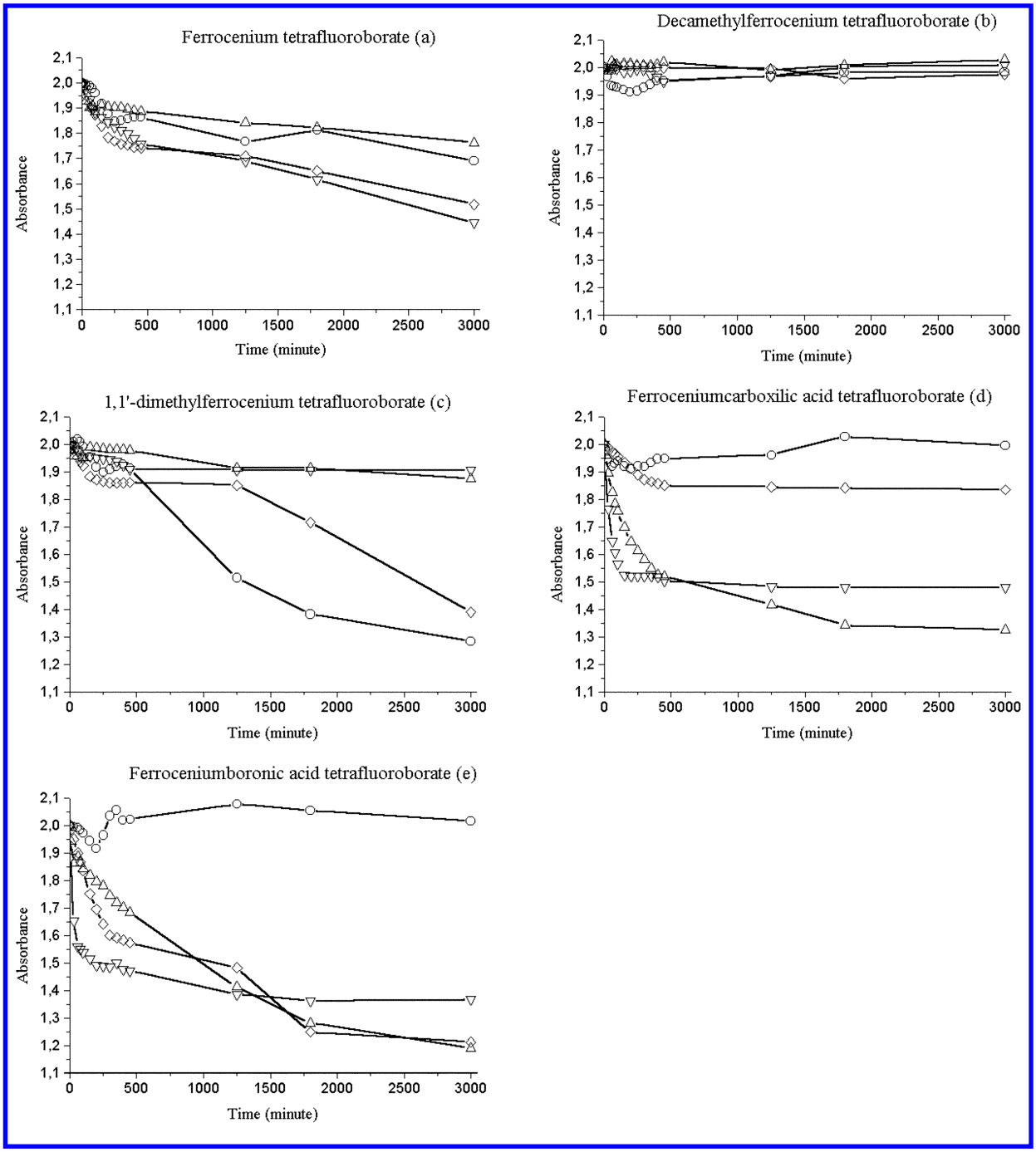

Figure 1. Stability of ferrocenium derivatives, $T = 25$ °C, in different buffers: (○) phosphate-citrate buffer, pH 3, i.e., citric acid 80 mM and disodium hydrogenphosphate (Na_2HPO_4) 40 mM. (◇) Distilled water, pH 6.0−6.5. (△) HEPES buffer 25 mM, pH 7.4. (▽) Phosphate buffer 65mM, pH 7.4. (a) Fc^+, time for decreasing of the maximum at $\lambda = 251$ nm, (b) $DEMFc^+$, time for decreasing of the maximum at $\lambda = 278$ nm, (c) $DIMFc^+$, time for decreasing of the maximum at $\lambda = 257$ nm, (d) $CAFc^+$, time for decreasing of the maximum at $\lambda = 257$ nm, (e) $BAFc^+$, time for decreasing of the maximum at $\lambda = 252$ nm.

environment of iron and the consequent interactions with the surrounding water molecules.

All the relaxation rates increased after 48 h except for that of $DEMFc^+$, thus confirming its stability in water.

Cytotoxicity Tests. The cytotoxicity of the five ferrocenium derivatives was evaluated on MCF-7 cell line. A first screening was accomplished through 48 h continuous treatments of cells with different concentrations of the compounds, ranging from 5 to 500 μM. The outcomes of this first screening revealed a general cytotoxic effect of the compounds, that leads to the total cell death for concentration values near 500 μM.

The $DEMFc^+$ showed the highest cytotoxic effect (IC_{50} of 37 μM), the other compounds having IC_{50} values around 300 μM (Table 2). $DEMFc^+$ revealed a good dose-activity relationship in the range between 5 and 100 μM. All of the other ferrocenium compounds showed negligible cytotoxic effects for concentration values up to 100 μM, and a maximum activity at 500 μM.

Further cytotoxicity tests were performed to focus on the time-exposure−activity relationship. In particular,

Table 1. Relaxation Measurements for Ferrocenium Compounds and for NaFe(III)EDTA and Na_2Fe(III)DTPA (temperature = 25 °C, frequency = 11.8 MHz)

compound	concn (M)	T_{1p} (s)	R_{1p} (s^{-1} M^{-1})	T_{1p} (s) (48 h)	R_{1p} (s^{-1} M^{-1}) (48 h)
Fc^+	1.0×10^{-2}	0.19	529	0.13	763
$DEMFc^+$	1.0×10^{-2}	1.25	80	1.23	81
$DIMFc^+$	1.0×10^{-2}	0.29	347	0.19	658
$CAFc^+$	1.0×10^{-3}	1.43	700	1.20	833
$BAFc^+$	5.0×10^{-3}	0.27	741	0.23	870
Fe(III)EDTA	2.0×10^{-2}	0.017	2996	–	–
Fe(III)DTPA	1.3×10^{-2}	0.072	1043	–	–

Table 2. In Vitro Cytotoxicity for MCF-7 of the Ferrocenium Derivatives[a]

compound	concentration (μM)	cell survival[b,c]	IC_{50} (μM)[b,d]
Fc^+	5	100% (25)	
	10	98% (27)	
	50	100% (15)	330 (26)
	100	99% (12)	
	500	13% (10)	
$DIMFc^+$	5	99% (16)	
	10	100% (19)	
	50	93% (13)	320 (19)
	100	90% (16)	
	500	17% (20)	
$DEMFc^+$	5	100% (18)	
	10	88% (10)	
	50	32% (13)	37 (15)
	100	10% (14)	
	500	11% (11)	
$CAFc^+$	5	100% (15)	
	10	98% (19)	
	50	97% (13)	340 (16)
	100	97% (10)	
	500	17% (13)	
$BAFc^+$	5	102% (20)	
	10	101% (17)	
	50	101% (14)	310 (17)
	100	98% (10)	
	500	8% (7)	

[a] Cells in the logarithmic phase of growth were treated for 48 h with concentrations ranging from 5 to 500 μM of the proper ferrocenium salt. After 48 h of drug exposure cells were counted by MTT method [b] Mean values of three replications. The limits of confidence ($P = 0.1$, $t = 2.92$) are reported in brackets. [c] Percentage of viable cells relative to the untreated control. [d] Concentration required to reduce to 50% the number of the cells with respect to the untreated control.

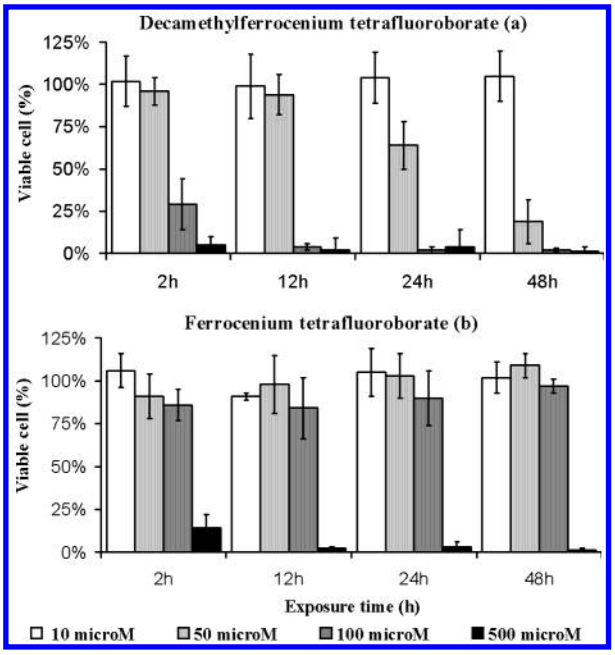

Figure 2. MCF-7 cell survival after 5 days of culture at different drug exposures (2, 12, 24, 48 h). The percentage of viable cells is referred to the control (not treated cells). Means from three independent experiments and limits of confidence ($P = 0.1$, $t = 2.92$) are reported. (a) $DEMFc^+$: 10, 50, 100, 500 μM. (b) Fc^+: 10, 50, 100, 500 μM.

Table 3. IC_{50} Values of $DEMFc^+$ and Fc^+ for MCF-7 Cytotoxicity Test[a]

compound	exposure time (h)	IC_{50} (μM)[b,c]
$DEMFc^+$	2	86 (11)
	12	74 (3)
	24	58 (13)
	48	35 (6)
Fc^+	2	308 (37)
	12	238 (34)
	24	256 (23)
	48	249 (10)

[a] Cells in the logarithmic phase of growth were incubated with the compounds for 2, 12, 24, 48 h. After the treatment, cells were washed with fresh medium and counted 5 days since the beginning of exposure [b] Mean values of three replications. The limits of confidence ($P = 0.1$, $t = 2.92$) are reported in brackets. [c] Concentration required to reduce to 50% the number of the cells with respect to the untreated control.

the behavior of $DEMFc^+$, the most active and stable complex, was compared with that of Fc^+. Five different concentrations of the two selected compounds were tested for increasing exposure times from 2 to 48 h. Cells were counted 5 days since the beginning of the exposure.

Data obtained from five day culture experiments confirmed the higher cytotoxic activity of $DEMFc^+$ in comparison with Fc^+, for all the drug exposure times tested (Figure 2 and Table 3). The decrease of the IC_{50} values for increasing exposure time indicated a good time-dependence of $DEMFc^+$ activity on this cell line. The almost constant IC_{50} values of Fc^+ suggests that the cytotoxic effect is limited to the first 12 h of treatment by the instability of Fc^+ itself.

Oxidative Damages on DNA Induced by DEM-Fc$^+$. The results obtained from the FACS measurement of 8-oxoguanine (8-oxoG), a direct marker of ROS attack on DNA in viable cells, clearly demonstrated that $DEMFc^+$ was able to increase the 8-oxo G level and to induce oxidative stress in the cells in a dose-dependent manner. This method provided a direct proof of the ROS activity in cells[11] thus supporting the findings obtained from the spin trapping experiments described below. Figure 3 shows a representative experiment of 8-oxoG presence in the cells.

Fc^+ in similar experimental conditions clearly caused a minor increase of 8-oxoG level with regard to $DEMFc^+$ (data not shown).

Decamethylferrocenium and Bleomycin. The cytotoxic activity of bleomycin on MCF-7 cell line was evaluated from 24 h treatment experiments. Cell survival was measured 5 days from the beginning of the treatment. It is noteworthy that the IC_{50} (53 μM)[16] was very close to the corresponding value for $DEMFc^+$ (58 μM, see Table 3), in the same experimental conditions.

To evaluate the potential synergy of the two compounds, MCF-7 cells were exposed to bleomycin for 24 h after a 24-h pretreatment with $DEMFc^+$. In this experiment the $DEMFc^+$ acts both as a cytotoxic compound and as a cofactor, supplying iron cations to the

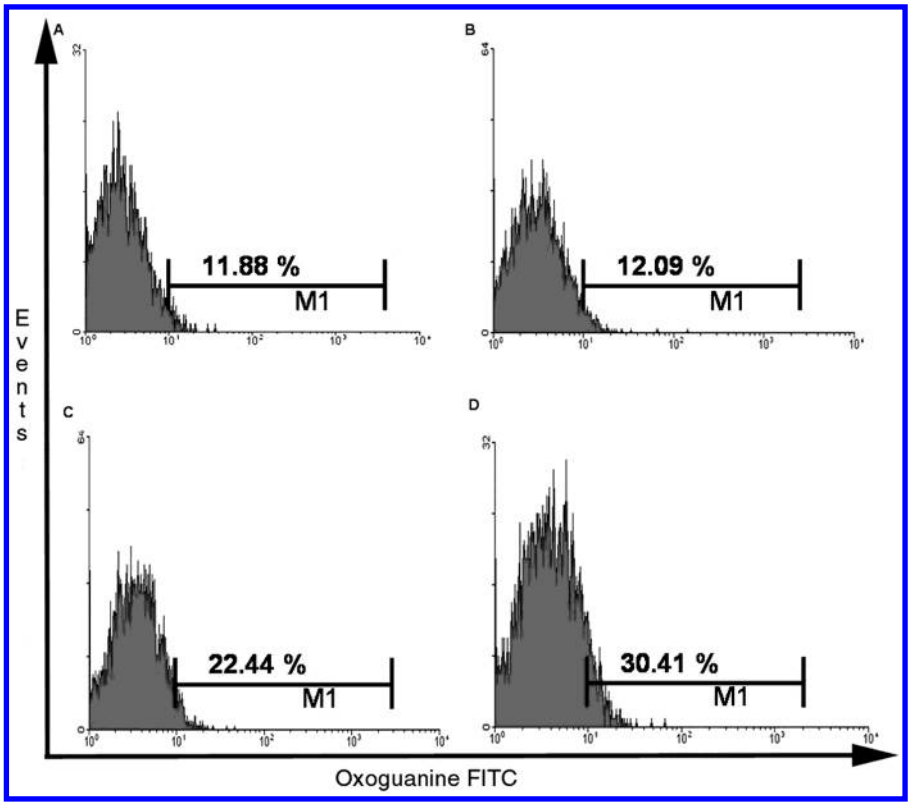

Figure 3. Flow cytometric analysis of the oxidative DNA damage induced by $DEMFc^+$ visualized with a specific probe for 8-oxo-G. After 30 min of treatment, cells were incubated with fresh media and harvested after 2 h. Paraformaldehyde fixed cells were incubated with the FITCH conjugate probe and fluorescence was measured with flow cytometry (FACS). The figure shows four univariate histograms of a representative experiment: cell number are expressed as number of events (*y* axis) versus 8-oxoG fluorescence intensity of FITCH-filter channel (*x* axis). Untreated cells are shown in panel A. Panels B, C, and D represent the 8-oxo-G moieties production (shift on *x* axis) due to the treatment with 10^{-6}, 10^{-5} and 10^{-4} M $DEMFc^+$ respectively and evidence a dose-dependent formation of oxidative DNA damages.

Table 4. Drug Combination vs Single Drug Experiments[a]

drug combination		$DEMFc^+$ (24 h treatment)		bleomycin	
concn (μM)	cell survival[b,c]	concn (μM)	cell survival[b,c]	concn (μM)	cell survival[b,c]
5 + 5	94% (15)	10	99% (15)	10	69% (7)
10 + 10	72% (13)	50	64% (14)	20	65% (8)
15 + 15	34% (12)	100	14% (2)	35	57% (3)
20+ 20	13% (10)	500	4% (10)	50	48% (5)
30 + 30	7% (10)			70	51% (7)
40 + 40	3% (8)				

[a] Drug combination cytotoxicity was tested utilizing $DEMFc^+$ and bleomycin in equimolar quantities. After 24 h of cell exposure to $DEMFc^+$, medium was replaced by fresh one containing bleomycin. Cells were cultured for further 24 h, in the presence of bleomycin, afterward the medium was replaced. Cells were counted by MTT method 5 days since the beginning of drug exposure. [b] Percentage of viable cells relative to the untreated control. [c] Mean values of three replications. The limits of confidence ($P = 0.1$, $t = 2.92$) are reported in brackets.

iron-dependent activation of bleomycin.[12] Different experiments were performed using equal $DEMFc^+$ and bleomycin concentrations, ranging from 5 to 40 μM. The value found for cell viability in the drug combination experiments, compared to those of the single components (see Table 4), roughly indicated a synergic effect. A more detailed analysis of the combined effect of multiple drugs has been proposed by Chou and Talalay.[17] Unfortunately, their method could not be applied here, because the dose−effect curves of the two drugs had different degrees of sigmoidicity.

Spin Trapping Studies. The ESR spectra at room temperature of samples containing the DEPMPO spin-trap (50 mM) and $DEMFc^+$ (0.67 mM) in HEPES buffer (25 mM) at pH 7.4 exhibited the signal pattern due to DEPMPO-OH adduct (*g* value 2.0059) ($a^N = 13.8$, $a^H = 13.8$, $a^P = 47.2$ G, Figure 4a)[18] which progressively increased in intensity. The spectra were complicated by the presence of a second pattern attributable to a carbon-centered radical adduct ($a^N = 14.3$, $a^H = 21.3$, $a^P = 46.0$ G) which began to appear at the same time. The same trend was observed using DMEM as media (containing HEPES 25 mM, see Figure 4b).

A sample containing the DMPO (50 mM) spin-trap and a lower concentration of $DEMFc^+$ (0.05 mM in phosphate buffer at pH 7.4 promptly showed the formation of the DMPO-OH adduct ($a^N = 14.9$, $a^H = 14.9$ G), whose intensity increased slowly with the time (Figure 5a−e). The six-line pattern of the carbon-centered radical adduct ($a^N = 15.4$, $a^H = 23.0$ G) began to appear evidently after 0.5 h of reaction, and it can be assigned to a cyclopentadienyl radical adduct.[19] A 0.05 mM

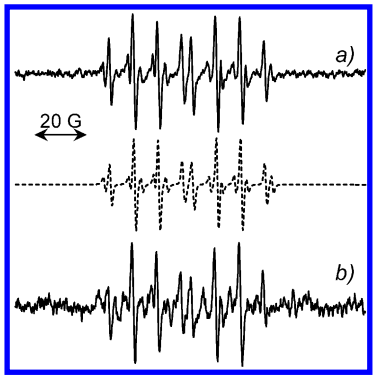

Figure 4. ESR spectra of buffered mixtures containing 50 mM DEPMPO and 0.67 mM $DEMFc^+$ incubated for 60 min using different media: (a) HEPES 25 mM pH 7.4; (b) DMEM. Simulated spectrum (dashed lines) was obtained by using: a^N = 13.8 G, a^H = 13.8 G, a^P = 47.2 G (hydroxyl adduct, 62%) and a^N = 14.3 G, a^H = 21.3 G, a^P = 46.0 G (carbon centered radical adduct, 38%). Instrument settings: modulation frequency, 100 kHz; modulation amplitude, 0.7 G; receiver gain 8×10^4; time constant, 163 ms; sweep rate, 145 G/min; microwave frequency, 9.77 GHz; microwave power, 20 mW, 20 scans.

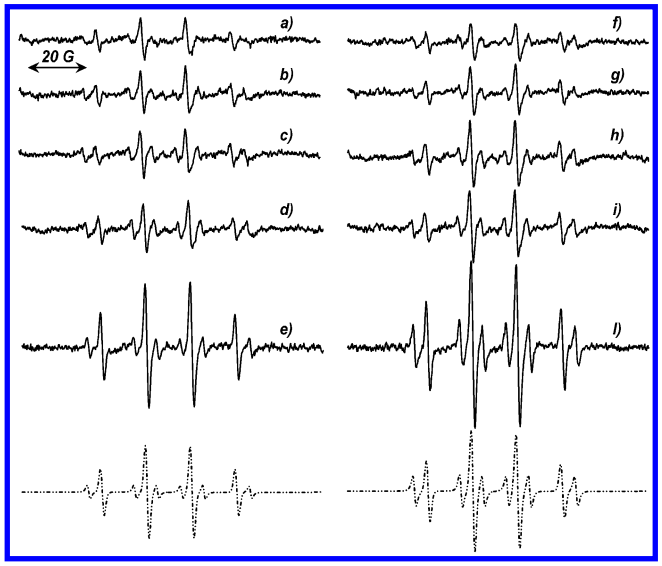

Figure 5. ESR spectra of phosphate-buffered mixtures (pH 7.4) containing 50 mM DMPO and either $DEMFc^+$ 0.05 mM (a−e) or Fc^+ 0.05 mM (f−l) incubated at different times: (a,e) 0 min; (b,f) 30 min; (c,g) 60 min; (d,h) 90 min; (e,l) 5 h. Simulated spectra (dashed lines) were obtained by using: a^N = 14.9 G, a^H = 14.9 G (hydroxyl adduct, 72% and 58%) and a^N = 15.4 G, a^H = 23.0 G (carbon-centered radical adduct, 28% and 42%, for $DEMFc^+$ and Fc^+ solutions, respectively). Instrument settings as in Figure 4.

solution of Fc^+ displayed the same trend but with higher relative intensities (Figure 5f−l).

Cyclopentadienyl derived radical species were also detected in the absence of spin trap. In fact, ESR spectra at 77 K of samples containing either $DEMFc^+$ or Fc^+ 0.67 mM in phosphate buffer pH 7.4 (Figure 6) showed a single line with ΔH_{pp} = 2 G in both cases, whose g values were 2.004 and 2.002, respectively.

Interestingly, all signal patterns disappeared when a reductant was present in the mixture. In fact, addition of ascorbate (1 mM) in the sample gave no trapped radicals even after 3 h, but the ascorbate doublet (1.8 G)[20] only.

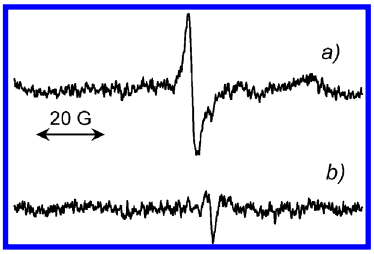

Figure 6. ESR spectra (77 K) of phosphate-buffered mixtures containing 50 mM DMPO and either $DEMFc^+$ 0.67 mM (a) or Fc^+ 0.67 mM (b) incubated for 30 min. Instrument settings: modulation frequency, 100 kHz; modulation amplitude, 0.7 G; receiver gain 8×10^4; time constant, 82 ms; sweep rate, 145 G/min; microwave frequency, 9.34 GHz; microwave power, 40 mW, 20 scans.

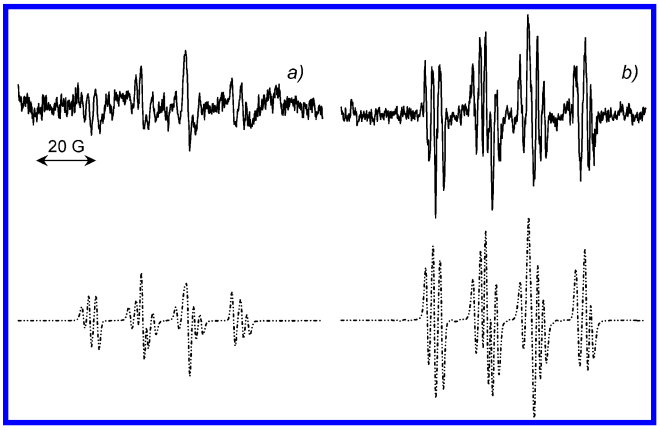

Figure 7. ESR spectra of phosphate-buffered mixtures containing 50 mM DMPO, sodium formate 67 mM and either $DEMFc^+$ 0.05 mM (a) or Fc^+ 0.05 mM (b) incubated for 30 min. Simulated spectra (dashed lines) were obtained by using: a^N = 14.9 G, a^H = 14.9 G (hydroxyl adduct, 29% and 27%), a^N = 15.6 G, a^H = 18.7 G (CO_2^- radical adduct, 51% and 42%) and a^N = 15.4 G, a^H = 23.0 G (carbon-centered radical adduct, 20% and 31%, for $DEMFc^+$ and Fc^+ solutions, respectively). Instrument settings as in Figure 4.

To determine if the detected hydroxyl radical adduct was formed exclusively by spin trapping of the hydroxyl radical rather than nucleophile addition of water to DMPO or decomposition of an hypothetical superoxide radical adduct, some ESR spectra were obtained on samples containing also sodium formate (67 mM). Both $DEMFc^+$ and Fc^+ showed the same trend supporting the evidence of a common reaction mechanism. In fact, three ESR patterns were found in both experimental series: the first pattern was due to the DMPO-CO_2 adduct (a^N = 15.6, a^H = 18.7 G),[21] the second one to a carbon-centered radical adduct (a^N = 15.5 a^H = 23.0 G) and finally the hydroxyl radical adduct pattern (Figure 7).

As sodium formate is a well-known scavenger of $^\bullet OH$, the presence of DMPO-CO_2 pattern confirms the existence of "genuine" $^\bullet OH$ radicals in solution.

To ascertain whether the formation of the hydroxyl radical adduct was O_2 dependent, samples were prepared and sealed under nitrogen. The corresponding spectra revealed the six-line pattern of the carbon-centered radical together with a very small signal due to DMPO-OH adduct (Figure 8a−c,f−h), thus supporting the hypothesis that dioxygen is involved in the formation of the hydroxyl radical, probably by a superoxide intermediate species. After slow diffusion of dioxygen into the same samples, the resulting ESR

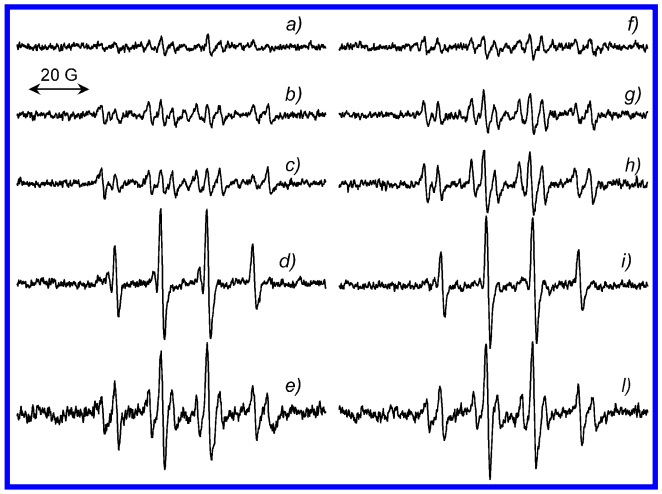

Figure 8. ESR spectra of phosphate-buffered mixtures containing 50 mM DMPO and either $DEMFc^+$ 0.05 mM (a−c) or Fc^+ 0.05 mM (f−h) incubated under nitrogen at different times: (a,f) 0 min; (b,g) 30 min; (c,h) 60 min. Spectra of samples opened after 5 h of incubation and kept in contact with air for 16 h: (d) $DEMFc^+$, 21 h; (i) Fc^+, 21 h. Spectra taken on fresh aerated samples after 90 min are given for comparison: (e) $DEMFc^+$, 90 min; (l) Fc^+, 90 min. Instrument settings as in Figure 4.

spectra (Figure 8d, 8i) showed the same DMPO-OH signal intensities as in fresh aerated samples (Figure 8e,l).

Evidence of the superoxide involvement was provided by the ESR spectra performed on a sample containing $DEMFc^+$ (0.05 mM), formate (0.1 M), catalase (CAT, 21,400 U/mL), and superoxide dismutase (SOD, 8,300 U/mL). These spectra showed the absence of any signal even after 1 h of reaction.

The ability of $DEMFc^+$ to oxidize cellular membrane lipids was tested by mixing $DEMFc^+$ (final concentration 0.05 mM), oleic acid (final concentration 12 mM), and DMPO (50 mM). The resulting ESR spectra showed two-carbon-centered radical adducts beside the presence of the hydroxyl radical adduct (Figure 9). The first carbon-centered adduct had $a^N = 15.5$, $a^H = 23.0$ G, whereas the second was characterized by $a^N = 16.1$, $a^H = 23.3$ G, which is compatible with a $^{\bullet}CR_3$ radical adduct coming from oxidation of a fatty acid.[22] Fc^+ produced similar, but more intense, signals (data not shown).

Discussion

The cytotoxicity tests confirmed the activity of the ferrocenium compounds. $DEMFc^+$ was an order of magnitude more cytotoxic than the other ferrocenium salts investigated (i.e., IC_{50} 37 μM vs 310−340 μM). Also the stability assays showed a peculiar behavior of this compound. Differently from the other salts, which revealed in the UV−vis studies a general instability in aqueous media, $DEMFc^+$ was stable in all the conditions tested.

The water relaxation rates indicated only an outer sphere coordination of the solvent molecules for all the ferrocenium solutions tested. The time evolution of the relaxation rates confirmed the order of stability found in the UV−vis studies, $DEMFc^+$ having the most stable R_{1p} value, almost constant over 48 h (see Table 1). These data are in agreement with a degradation mechanism that involves directly the solvent molecules, as previously asserted by Prins et al.[13] The initial degradation of ferrocenium derivatives in the presence of a nucleophilic solvent, (e.g. water), can account for the formation of Fe(II) species:

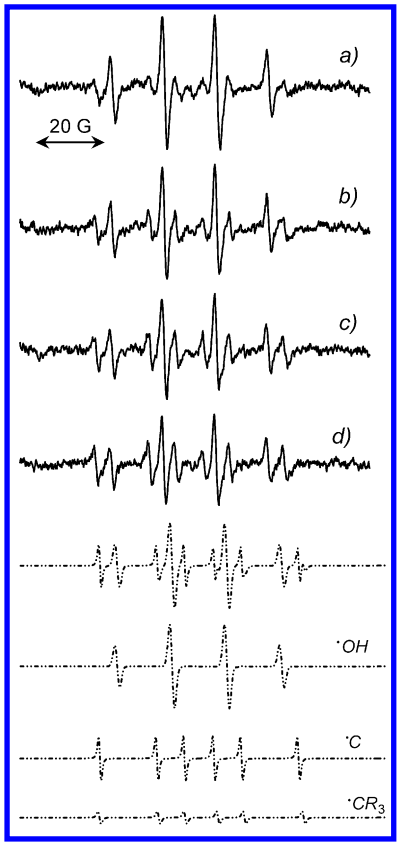

Figure 9. ESR spectra of phosphate-buffered mixtures containing 50 mM DMPO, oleic acid 20 mM and either $DEMFc^+$ 0.67 mM incubated at different times: (a) 0 min; (b) 30 min; (c) 60 min; (d) 90 min. Simulated spectrum (dashed line) was obtained by using: $a^N = 14.9$ G, $a^H = 14.9$ G (hydroxyl adduct, 62%), $a^N = 16.1$ G, $a^H = 23.3$ G (CR_3 radical adduct, 9%) and $a^N = 15.5$ G, $a^H = 23.0$ G (carbon centered radical adduct, 28%).

$$2[Fe^{III}Cp_2]^+ + nH_2O \rightarrow [Fe^{II}(H_2O)_n]^{2+} + [Fe^{II}Cp_2] + 2Cp^{\bullet} \quad (1)$$

The ESR signal pattern due to hydroxyl radical adduct, obtained when a ferrocenium derivative is dissolved in aqueous media, suggests the occurrence of an Haber−Weiss-like cycle(2−3)[23,24] which ends with the Fenton reaction (4) generating $^{\bullet}OH$.[25]

$$[Fe^{II}(H_2O)_n]^{2+} + O_2 \rightarrow [Fe^{III}(H_2O)_n]^{3+} + O_2^{\bullet -} \quad (2)$$

$$2O_2^{\bullet -} + 2H_2O \rightarrow O_2 + H_2O_2 + 2OH^- \quad (3)$$

$$[Fe^{II}(H_2O)_n]^{2+} + H_2O_2 \rightarrow [Fe^{III}(H_2O)_n]^{3+} + OH^- + {}^{\bullet}OH \quad (4)$$

We are aware that in the presence of iron salts, the DMPO-OH adduct can be formed by a nucleophilic addition of water to DMPO. This possibility has been checked by running some ESR spectra in the presence of hydroxyl radical scavengers. The partial scavenging of the hydroxyl radical and the appearance of the

DMPO−CO_2 adduct in the spectra, obtained with the addition of formate to the samples, excludes that hydroxyl radical adduct signal coming exclusively from a nucleophilic addition of water to the spin trap.

The persistence of a hydroxyl radical adduct signal in the presence of formate, can be due to the decomposition of DMPO-OOH adduct, whose half-life is about one minute at pH 7.4.[26] Even when DEPMPO was used in place of DMPO, no signal attributable to a superoxide adduct was detected, although the half-life of the DEPMPO-OOH adduct is about 15 times longer than that of the DMPO-OOH adduct.[18] This behavior can be explained by taking into account that the superoxide radical undergoes spontaneous dismutation reaction (see reaction 3), whose rate is about 2.4×10^5 M^{-1} s^{-1} at pH 7.4.[27]

ESR spectra of samples prepared and managed under nitrogen showed that DMPO-OH signal intensities were greatly decreased in comparison to those obtained from similar samples prepared in air. Interestingly, these same samples on standing in contact with air in the quartz flat cell produced, after some hours, ESR intensities which became comparable to those coming from the samples prepared in air. When SOD and CAT were added in the preparation of the sample, only noise was recorded. All these results proved that dioxygen was involved in the formation of superoxide radical, whose spin trap adduct rapidly decomposed, giving the corresponding hydroxyl adduct. The latter was actually observed in the accumulation of a full ESR experiment, and it is due to both "genuine" hydroxyl radical and degraded DMPO-OOH adducts.

A carbon-centered radical adduct attributable to a cyclopentadienyl radical was evidenced in the ESR spectra. Even though the degradation pathway of ferrocenium compounds in water accounts for the formation of the $Cp^{\bullet}$ radical, we believe this species rearranges too rapidly[28] to be spin trapped. Probably, the Cp-derived adduct can be assigned to a secondary cyclopentadienyl radical produced by reaction of the hydroxyl radical with the (bonded or free) R_5Cp. Evidence of the presence of Cp-oxygen radicals comes from low-temperature ESR spectra in the presence of air, where the singlets observed have been attributed to $R_5CpOO^{\bullet}$ radicals (see Figure 6).[28] This hypothesis is also supported by the ESR spectra in the presence of CAT and SOD, where the suppression of the oxygen radicals caused the disappearance of the carbon-centered radical signals too.

The complete quenching of all ESR spin trap signals by addition of ascorbate to the sample can be easily explained considering that ascorbate competes very efficiently with DMPO for both superoxide and hydroxyl radical,[29] thus producing the ascorbyl radical which is the only radical species observed.

Kirsch et al.[30] claimed the formation of hydrogen peroxide in HEPES containing buffers, when peroxynitrite is formed in the bulk. These authors stated that any oxidant strong enough to oxidize certain tertiary amines (such as HEPES) in one-electron step would be able to initiate a reaction sequence leading to the formation of hydrogen peroxide. Conversely, Simpson et al.[31] stated that HEPES "showed a biphasic dependence on concentration: low concentrations (2.5−10 mM) stimulated the response in a dose-related fashion, and high concentrations (20 mM) inhibited completely". In addition, "HEPES in a radical-generating system is normally considered a radical scavenger" as stated by the same authors. The results presented in this work did not showed any appreciable variation in the ESR spectrum intensities when HEPES was used as media. Moreover, the data obtained in HEPES and DMEM match those obtained in phosphate buffer. It is quite reasonable to assume that in our experimental condition the mechanism stated by Kirsch et al. might not occur. On the other hand, the added spin trap (DEMPO or DMPO) should be much more easily oxidizable than HEPES. Such oxidation would lead to a 2,2′-DMPO-like dimer formation,[32] which was not observed. Therefore, our results should be unaffected by the production of hydrogen peroxide due to reaction of HEPES with oxidants, as confirmed by data obtained in phosphate buffer.

The addition of oleic acid in the sample resulted in an additional feature in the ESR spectra. The simulation of the spectrum taken after 90 min reveals a contribution of the lipid derived DMPO adduct.

Conclusions

The toxicity of ferrocenium derivatives in our in vitro model is due to oxidative damage to DNA. This study outlines the stability−cytotoxicity relationship for this class of compounds: the most stable compound, namely $DEMFc^+$, is actually the most cytotoxic. The lower degradation rate of $DEMFc^+$ and its higher lipophilicity (compared with the other ferrocenium salts tested) allow the diffusion of a larger amount of "intact" molecules into the cell, where they produce $^{\bullet}OH$ radicals. An extracellular cytotoxic effect is suggested for all the other unstable salts, supported also by the short time occurring for the cell killing, and the more intense lipid oxidation (ESR data on Fc^+) suggestive of an external membrane damage. This mechanism is evident only for high concentrations, where the inflicted damage is sufficient to cause cell death. On the contrary, the $DEMFc^+$ toxicity is time- and dose-dependent, as evident for prolonged treatments.

The proposed mechanism of action of $DEMFc^+$ justifies the rationale for its combination with the iron-dependent drug bleomycin. The synergistic effect found in a physiological range of concentrations highlights the pharmacological potentiality of the former compound. In fact, FACS shows the ability of $DEMFc^+$ of inflicting oxidative damage of the guanine nucleobase, whereas bleomycin mainly affect the sugar residues with a fully complementary mechanism of oxidative stress of DNA. Moreover the iron ions made available from $DEMFc^+$ decomposition can be incorporated in bleomycin, further improving its activity.

Since there is an enormous body of knowledge on the synthesis of ferrocene derivatives,[33] the opportune choice of ring substituents will trigger the stability level of the corresponding cations toward the maximal cytotoxic effect, and possibly toward selectivity. Indeed, recent research activity has been focused on the synthesis of stable, water-soluble, ferrocenium derivatives to be tested as antitumor agents.[34,35]

Experimental Section

Reagents and Instrumentation. Ferrocene $Fe[(\eta^5\text{-}C_5H_5)]_2$, decamethylferrocene $Fe[(\eta^5\text{-}C_5(CH_3)_5)]_2$, 1,1′-dimethylferrocene $Fe[(\eta^5\text{-}C_5H_4CH_3)]_2$, ferrocenecarboxylic acid $Fe[(\eta^5\text{-}C_5H_5)(\eta^5\text{-}C_5H_4COOH)]$, and ferroceneboronic acid $Fe[(\eta^5\text{-}C_5H_5)(\eta^5\text{-}C_5H_4B(OH)_2)]$ were purchased from Aldrich, bleomycin A_2 from Xechem. Reagent grade organic solvents were purchased from Aldrich and used as received. $AgBF_4$ 98% from Strem Chemicals was used as the oxidizing agent. UV−vis spectra were recorded on a Perkin-Elmer Lambda 20 spectrophotometer. Measurements of longitudinal water proton relaxation rates were carried out on a desktop MS5-M spectrometer (Institute Jozef Stefan, Ljubljana, Slovenia) operating at the magnetic field strength of 0.28 T (corresponding to a proton Larmor frequency of 11.8 MHz). IR spectra were recorded using KBr pellets in the 4000−400 cm^{-1} range on a Bruker Equinox 55 FT-IR spectrophotometer at a 4 cm^{-1} resolution and coadding 16 scans. Electrospray mass spectra (ESI-MS) were obtained by a Micromass ZMD mass spectrometer. Typically, a dilute solution of compound in water was delivered directly to the spectrometer source at 0.01 cm^3 min^{-1}, using a Hamilton gastight microsyringe controlled by a single-syringe infusion pump. The nebulizer tip was at 3000−3500 V and 150 °C, with nitrogen used both as a drying and a nebulizing gas. The cone voltage was usually 30 V, when clean parent ions were required, and was varied up to 130 V to investigate fragmentation processes. Molecular ion peaks were assigned from the *m*/*z* values and from the simulated isotope distribution patterns. Elemental analysis results for elements indicated by symbols were within ±0.4% of theoretical values. Electron spin resonance (ESR) spectroscopic measurements were carried out on a Bruker ER 200 D spectrometer driven by an ESP 3220 data system and equipped with an NMR gaussmeter. Spin trapping experiments were recorded at room temperature in a standard quartz flat cell. ESR spectra at room temperature (spin trap adducts) were simulated by using PEST Winsim developed by D. R. Duling.[36] Frozen solution spectra were recorded at 77 K.

Preparation of Ferrocenium Salts. $AgBF_4$ was added stoichiometrically to 10 mL of an acetone solution containing the ferrocene. A dark gray precipitate appeared immediately. The reaction mixture was filtered to remove metallic silver. The filtered solution was evaporated, and the solid product was dried under vacuum.

Ferrocenium tetrafluoroborate (Fc^+). Yield: 92%. Anal. ($C_{10}H_{10}BF_4Fe$) C, H, Fe. IR (KBr, cm^{-1}): 3100 s (C−H), 1415 m (C−C), 1105 vs, 851 s (CH), 816 m (CH), 490 w, 477 w. ESI-MS: *m*/*z* 186 $[M]^+$.

Decamethylferrocenium tetrafluoroborate ($DEMFc^+$). Yield: 91%. Anal. ($C_{20}H_{30}BF_4Fe$) C, H, Fe. IR (KBr, cm^{-1}): 2982 w (CH_3), 2962 w (CH_3), 2908 mw (CH_3), 1475 m (Cp−CH_3), 1460 sh (Cp−CH_3), 1381 ms (Cp−CH_3), 1423 w (C−C), 1094 vs, 591 w, 450 w (Cp−Fe−Cp). ESI-MS: *m*/*z* 326 $[M]^+$.

1,1′-Dimethylferrocenium tetrafluoroborate ($DIMFc^+$). Yield 89%. Anal. ($C_{12}H_{14}BF_4Fe$) C, H, Fe. IR (KBr, cm^{-1}): 3105 s (C−H), 2963 m (CH_3), 2924 m (CH_3), 2854 m (CH_3), 1477 m (Cp−CH_3), 1391 mw (Cp−CH_3), 1450 m (C−C), 1113 sh, 853 m (CH), 482 w. MS-ESI: *m*/*z* 214 $[M]^+$.

Ferroceniumcarboxylic acid tetrafluoroborate ($CAFc^+$). Yield 85%. Anal. ($C_{11}H_{10}O_2BF_4Fe$) C: calcd, 41.70; found, 42.07; H, Fe. IR (KBr, cm^{-1}): 3180 sbr (O−H), 3118 s (C−H), 2632 m (C═O), 2554 m (C═O), 1706 vs (C═O), 1653 vs (C═O), 1475 s, 1415 m (OH), 1400 m (OH), 1295 s (C−O), 1283 sh (C−O), 1109 s, 914 w (OH), 858 m (CH), 483 mw. ESI-MS: *m*/*z* 230 $[M]^+$.

Ferroceniumboronic acid tetrafluoroborate ($BAFc^+$). Yield 82%. Anal. ($C_{10}H_{11}O_2B_2F_4Fe$) C, H; Fe: calcd, 17.64; found, 17.38. IR (KBr, cm^{-1}): 3217 vs br (BOH), 3104 s (C−H), 1460 s (C−C), 1380 ms (B−O), 1202 s (B−C), 857 m (CH), 636 m, ESI-MS: *m*/*z* 230 $[M]^+$.

UV−vis Spectra. Solutions were prepared for each ferrocenium salt, adjusting the absorbance value at 250 nm in a range between 1 and 2 absorbance units. With filtered solutions, the UV−vis spectra were recorded, and the absorbance value of the maximum in the region between 200 and 300 nm was considered as the starting value for stability tests. For each spectrum the maximum absorbance value was baseline corrected.

Relaxation Measurements. T_1 values were measured with 180°−90° method (inversion recovery) at 11.8 MHz and 25 °C. The longitudinal net molar relaxation rate (R_{1p}) is given by: $R_{1p} = \{[\text{paramagnetic species}]T_{1p}\}^{-1}$ where $(T_{1p})^{-1} = T_1(\text{observed})^{-1} - T_1(\text{blank})^{-1}$ and T_1(blank) is the longitudinal relaxation time for distilled water (2.37 s). Salts were dissolved in distilled water (pH 6−6.5) at the molar concentration reported in Table 1. The reference salts NaFe(III)EDTA and Na_2Fe(DTPA) were synthesized according to literature methods.[37,38] The solutions of NaFe(III)EDTA[39] and Na_2Fe(III)-DTPA[40] were adjusted to pH 5 and 9, respectively, at which each complex is stable.

Cytotoxicity Tests. General Procedures. Human breast adenocarcinoma (MCF-7) cells were cultured in DMEM culture media (with HEPES 25 mM) containing L-glutamine (2 mM) supplied with 10% of fetal calf serum (FCS) (Sigma) and incubated under standard conditions (37 °C, 5% CO_2) in plastic culture flask. All experiments were carried out using cells in the exponential phase of growth. Cells were trypsinized, resuspended in DMEM containing 10% FCS and seeded (250000 cells/well) in 6-well plates. After 24 h the medium was replaced by fresh medium containing the drug. Fresh complete medium without drugs was used for controls. At the end of the treatment, cell viability was evaluated measuring the activity of the mitochondrial enzyme succinate dehydrogenase. This test used 3-(4,5-dimethylthiazol-2-yl)-2,5-diphenyltetrazolium bromide (MTT) (Sigma) as substrate that was converted to a formazan product, which was detected spectrophotometrically at 570 nm using a 690 nm background correction.

First Screening Test. Cells were treated for 48 h with concentrations ranging from 5 to 500 μM of the proper ferrocenium salt. A control culture was used for each ferrocenium salt tested. After 48 h of drug exposure, MTT solution of 5 mg/mL (in saline) was added in each well, and cells were incubated for 60 min. The medium was carefully removed to eliminate the dye excess, and the formazane product was dissolved with acidified isopropyl alcohol (0.12 M HCl). The percentage cell viability was calculated by the equation:

$$\text{cell viability (\%)} = \frac{A_{570}^{\text{test}} - A_{690}^{\text{test}}}{A_{570}^{\text{ctrl}} - A_{690}^{\text{ctrl}}} \cdot 100$$

Decamethylferrocenium vs Ferrocenium Cytotoxicity Assay. $DEMFc^+$ and Fc^+ were tested at 10, 50, 100, 500 μM concentrations with different drug exposure times. In every single experiment cells were exposed to the same concentration of the two drugs for increasing times (2, 12, 24, and 48 h). Cells were treated with the two compounds after 24 h of growth. An untreated control for each treatment time was added. At every time point, medium was replaced by fresh one in the corresponding well (test and control). Cells were always counted 5 days since the beginning of the treatment with the same method described for the first screening. The percentage cell viability was calculated considering the control that was washed at the corresponding time:

$$\text{cell viability (\%)} = \frac{A_{570}^{\text{test time (X)}} - A_{690}^{\text{test time (X)}}}{A_{570}^{\text{ctrl time (X)}} - A_{690}^{\text{ctrl time (X)}}} \times 100$$

Detection of Oxidative Damage to Cellular DNA in Vitro. The oxidative damages on DNA, due to the generation of intracellular reactive oxygen species (ROS), have been investigated by measuring the presence of 8-oxoguanine residues with a specific fluorescent probe. Cells were trated for 30 min with $DEMFc^+$ dissolved in complete media at concentrations of 10^{-4}, 10^{-5}, and 10^{-6} M, washed twice with fresh media, incubated for 2 h with fresh media, finally harvested, fixed with 2% ice-cold parafolmaldehyde, and treated with 70% ethanol. The detection of 8-oxoguanine was

performed by using Fluorogenic OxyDNA Assay kit (Calbiochem, CA). The FITC-labeled conjugate evidenced radical-derived DNA products, and the quantification was performed with a FACSCalibur System and CellQuest software (Becton-Dickinson, NJ).

Decamethylferrocenium and Bleomycin. Bleomycin A_2 was tested on MCF-7 cell line at 10, 20, 35, 50, 70 μM concentrations. After 24 h of drug exposure, the medium was replaced by fresh one and cell viability was evaluated by MTT method, 5 days since the beginning of the treatment. Drug combination cytotoxicity was tested at the concentrations reported in Table 4, utilizing $DEMFc^+$ and bleomycin in equimolar quantities. After 24 h of cell exposure to $DEMFc^+$, medium was replaced by fresh one containing bleomycin. Cells were cultured for further 24 h, in the presence of bleomycin, afterward the medium was replaced. Cells were counted by MTT method 5 days since the beginning of drug exposure. The percentage cell viability was calculated considering the untreated control.

Spin Trapping Measurements. Spin trapping experiments were carried out to identify which radicals are produced when the ferrocenium derivatives are dissolved in aqueous media. 5,5-Dimethyl-1-pyrroline *N*-oxide (DMPO) was purchased from Sigma and used after vacuum distillation to remove orange paramagnetic impurities present in the commercial samples. 5-(Diethoxyphosphoryl)-5-methyl-1-pyrroline *N*-oxide (DEPMPO)[18,41] was purchased from Oxis and used without any further purification. The spin trap reagent was dissolved in each solution before the addition of the proper ferrocenium derivative. The reaction mixtures for spin trap experiments were prepared by adding 100 μL of the proper ferrocenium derivative (2 mM or 0.15 mM) to 200 μL of aqueous media. The aqueous media mainly used were phosphate buffer (PB) 0.1 M, pH 7.4; HEPES 25 mM, pH 7.4, and culture media DMEM (with HEPES 25 mM, Sigma). Most of the measurements were run by using ferrocenium solutions, 0.15 mM (final concentration 50 μM), in order to rule out any interference with the spin trap. In fact, ferrocenium derivatives can oxidize DMPO to 2,2′ DMPO dimer[32] ($a^N = 14.5$, $a^H = 16.0$ G, not shown) if added at sufficient high concentration. Several spectra were recorded for each reaction mixture at different times, to follow the evolution of the signals of the trapped radicals.

Acknowledgment. MIUR (Rome), CNR (Rome) and CIRCMSB (Bari) are gratefully acknowledged for financial support. The research was carried out in the frame of the EU COST D20 action (metal compounds in the treatment of cancer and viral diseases). We thank Prof. M. Botta and Dr. M. Ravera (Università "A. Avogadro") for the T_1 measurements and electrospray mass spectra, respectively. We are indebted to a reviewer for having greatly improved the manuscript.

References

(1) Köpf-Maier, P.; Köpf, H. Non-platinum-group Metal Antitumor Agents: History, Current status, and Perspectives. *Chem. Rev.* **1987**, *87*, 1137−1152

(2) Köpf-Maier, P.; Köpf, H.; Neuse, E. W. Ferricenium Complexes: a New Type of Water-soluble Antitumor Agent. *Cancer Res. Clin. Oncol.* **1984**, *108*, 336−340.

(3) Motohashi, N.; Meyer, R.; Gollapudi, S. R.; Bhattiprolu, K. R. Synthesis and Activity of Potential Antitumor Ferrocenes. *J. Organomet. Chem.* **1990**, *398*, 205−217

(4) Neuse, E. W.; Kanzawa, F. Evaluation of The Activity of Some Water-soluble Ferrocene and Ferricenium Compounds. Against Carcinoma of the Lung by The Human Tumor Clonogenic Assay. *Appl. Organomet. Chem.* **1990**, *4*, 19−26.

(5) Osella, D.; Ferrali, M.; Zanello, P.; Laschi, F.; Fontani, M.; Nervi, C.; Cavigiolio, G. On The Mechanism of the Antitumor Activity of Ferrocenium Derivatives. *Inorg. Chim. Acta* **2000**, *306*, 42−48.

(6) Köpf-Maier, P.; Klapötke, T. Tumor Inhibition by Ferricenium Complexes. *Arzneim.-Forsch.* **1989**, *39* (I), 369−371.

(7) Köpf-Maier, P. Tumor Inhibition by Ferricenium Complexes: Systemic Effect in Vivo and Cell Growth Inhibition in Vitro. *Z. Naturforsch., C: Biosci.* **1985**, *40*, 843−846.

(8) Houlton, A.; Roberts, R. M. G.; Silver, J. Studies on the Antitumour Activity of Some Iron Sandwich Compounds. *J. Organomet. Chem.* **1991**, *418*, 107−112.

(9) Wenzel, M.; Wu, Y.; Liss, E.; Nuse, E. W. Stability of Ferricinium and its Cytostatic Effect. *Z. Naturforsch., C: Biosci.* **1988**, *43c*, 963−966.

(10) Tamura, H.; Miwa, M. DNA Cleaving Activity and Cytotoxic Activity of Ferrocenium Cations. *Chem. Lett.* **1997**, 1177−1178.

(11) De Zwart, L. L.; Meerman, J. H. N.; Commandeur, J. N. M.; Vermeulen, N. P. E. Biomarkers of Free Radical Damage Applications in Experimental Animals and in Humans. *Free Radical Biol. Med.* **1999**, 26, 202−226.

(12) Burger, R. M. Cleavage of Nucleic Acids by Bleomycin. *Chem. Rev.* **1998**, *98*, 1153−1169.

(13) Prins, R.; Korswagen, A. R.; Kortbeek, A. G. T. G. Decomposition of the Ferricenium Cation by Nucleophilic Reagents. *J. Organomet. Chem.* **1972**, *39*, 335−344.

(14) Shon, R. B.; Hendrickson, D. N.; Gray, H. B. Electronic Structure of Metallocenes. *J. Am. Chem. Soc.* **1971**, *93*, 3603−3612.

(15) Lauffer, R. B. Paramagnetic Metal Complexes as Water Proton Relaxation Agents for NMR Imaging: Theory and Design. *Chem. Rev.* **1987**, *87*, 901−927.

(16) Hait, W. N.; Gesmonde, J. F.; Lazo, J. S. Effect of Anticalmodulin Drugs on the Growth and Sensitivity of C6 Rat Glyoma Cells to Bleomycin. *Anticancer Res.* **1994**, *14*, 1711−1721.

(17) Chou, T. C.; Talalay, P. Quantitative Analysis of Dose−effect Relationships: the Combined Effects of Multiple Drugs or Enzyme Inhibitors. *Adv. Enzyme Regul.* **1984**, *22*, 27−55.

(18) Frejaville, C.; Karoui, H.; Tuccio, B.; Le Moigne, F.; Culcasi, M.; Pietri, S.; Lauricella, R.; Tordo, P. 5-(Diethoxyphosphoryl)-5-methyl-1-pyrroline N−Oxide: A New Efficient Phosphorylated Nitrone for the in Vitro and in Vivo Spin Trapping of Oxygen-Centered Radicals. *J. Med. Chem.* **1995**, *38*, 258−265.

(19) Barker, P. J.; Stobart, S. R.; West, P. R. Spin Trapping of Cyclopentadienyl Radicals using Nitroso Compounds and Nitrones. *J. Chem. Soc., Perkin Trans. 2* **1986**, 127−130.

(20) Bernofsky, C.; Bandara, B. M. Spin Trapping Endogenous Radicals in MC-1010 Cells: Evidence for Hydroxyl Radical and Carbon-centered Ascorbyl Radical Adducts. *Mol. Cell. Biochem.* **1995**, *148*, 155−164.

(21) Buettner, G. R. Spin Trapping: ESR Parameters of Spin Adducts. *Free Radical Biol. Med.* **1987**, *3*, 259−303.

(22) Dikalov, S. I.; Mason, R. P. Spin Trapping of Polyunsaturated Fatty Acid-derived Peroxyl Radicals: Reassignment to Alkoxyl Radical Adducts. *Free Radical Biol. Med.* **2001**, *30*, 187−197.

(23) Minotti, G.; Aust, S. D. The Requirements for The Iron(III) in The Initiation of The Lipid Peroxidation by Iron(II) and Hydrogen Peroxide. *J. Biol. Chem.* **1987**, *262*, 1098−1104.

(24) Minotti, G.; Aust, S. D. Redox Cycling of Iron and Lipid Peroxidation. *Lipids* **1992**, *27*, 219−226.

(25) Goldstein, G.; Meyerstein, D.; Czapski, G. The Fenton Reagents. *Free Radic. Biol. Med.* **1993**, *15*, 435−445.

(26) Buettner, G. R.; Oberley, L. W. Considerations in The Spin Trapping of Superoxide and Hydroxyl Radical in Aqueous Systems Using 5,5Dimethyl-1-pyrroline-1-oxide. *Biochem. Biophys. Res. Commun.* **1978**, *83*, 69−74.

(27) Bielski, B.; Cabelli, D. E. Highlights of Current Research Involving Superoxide and Perhydroxyl Radicals in Aqueous Solutions. *Int. J. Radiat. Biol.* **1991**, *59*, 291−319.

(28) Davies, A. G.; Lusztyk, J. Photolysis of the Carbon−Hydrogen Bond in Pentamethylcyclopentadiene. Properties of the Pentamethylcyclopentadienyl Radical. *J. Chem. Soc., Perkin Trans. 2* **1981**, 692−696.

(29) Tabbì, G.; Fry, S. C.; Bonomo, R. P. E. S. R. Study of Nonenzymic Scission of Xyloglucan by an Ascorbate-H_2O_2-copper System: The Involvement of The Hydroxyl Radical and The Degradation of Ascorbate. *J. Inorg. Biochem.* **2001**, *98*, 1153−1169.

(30) Kirsch, M.; Lomonosova, E. E.; Korth, H.-G.; Sustmann, R.; de Groot, H. Hydrogen Peroxide Formation by Peroxynitrite with HEPES and Related Tertiary Amines. *J. Biol. Chem.* **1998**, *273*, 12716−12724.

(31) Simpson, J. A.; Cheeseman, K. H.; Smith, S. E.; Dean, R. T. Free Radical Generation by Copper Ions and Hydrogen Peroxide. *Biochem. J.* **1988**, *254*, 519−523.

(32) Thornalley, P. J. The Haemolitic Reactions of 1-Acetyl-2-Phenylhydrazine and Hydrazine: a Spin Trapping Study. *Chem.-Biol. Interact.* **1984**, *50*, 339−349.

(33) Robert, C. K. In *Comprehensive Organometallic Chemistry II*; Abel, E. W., Gordon, F., Stone, A., Wilkinson, G., Eds.; Pergamon: Oxford, 1995; Vol. 7 Chapter 2.8, pp 185−198.

(34) Bradley, S.; McGowan, P. C.; Oughton, K. A.; Thornton-Pett, M.; Walsh, M. E. Facile Synthesis of Amino-functionalised Ferrocenes and Vanadocenes. *Chem. Commun.* **1999**, 77−78.

(35) Bradley, S.; Camm, K. D.; Liu, X.; McGowan, P. C.; Mumtaz, R.; Oughton, K. A.; Podesta, T. J.; Thornton-Pett, M. Synthesis and Structural Studies of 1,1′-Bis-Amino-Functionalized Ferrocenes, Ferrocene Salts, and Ferrocenium Salts. *Inorg. Chem.* **2002**, *41*, 715−726.
(36) Duling, D. R. Simulation of Multiple Isotropic Spin Trap EPR Spectra. *J. Magn. Reson.* **1994**, *B 104*, 105−110.
(37) Lind, M. D.; Hoard, J. L.; Hamor, M. J.; Hamor, T. A. Stereochemistry of Ethylenediaminetetraacetato Complexes. *Inorg. Chem.* **1964**, *3*, 34.
(38) Hall, L. H.; Spijkerman, J. J.; Lambert, J. L. Preparation and Coordination Studies of the Complex Acid, Dihydrogen Diethylenetriaminepentaacetatoferrate(III) Dihydrate, and Several of Its Metal(I) Salts. *J. Am. Chem. Soc.* **1968**, *90*, 2044−2048.
(39) Bloch, J.; Navon, G. A Nuclear Magnetic Resonance Relaxation Study of Iron(III) EDTA in Aqueous Solution. *J. Inorg. Nucl. Chem.* **1980**, *42*, 693−699.
(40) Oakes, J.; van Karlingen, C. G. Spectroscopic Studies of Transition-metal Ion Complexes of Diethylenetriaminepenta-acetic Acid and Diethylenetriamine-penta-methylphosphonic Acid. *J. Chem. Soc., Dalton Trans.* **1984**, 1133−1137.
(41) Vásquez-vivar, J.; Hogg, N.; Pritchard, K. A.; Martasek, K. P.; Kalyanaraman, B. Superoxide Anion Formation from Luigenin: an Electron Spin Resonance Spin-trapping Study. *FEBS Lett.* **1997**, *403*, 127−130.

JM021003K